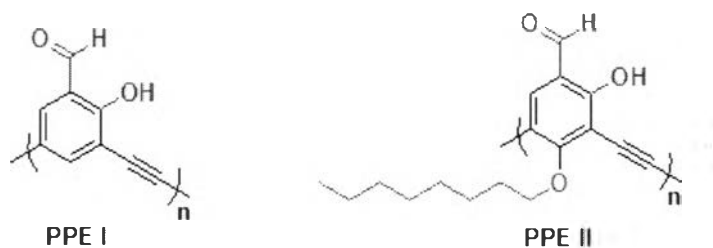


## CHAPTER III

### Results and Discussion

#### 3.1 Cyanide fluorescence sensors from poly(phenyleneethynylene)s (PPEs) : PPE I, PPE II, PPE III, and PPE IV

In this research, we designed and synthesized the fluorophore PPE I – PPE IV containing poly(phenylene ethynylene) as a fluorogenic unit and salicylaldehyde group as cyanide ion receptor (Figure 3.1). The salicylaldehyde were attached in all polymer (PPE I, PPE II, PPE III, and PPE IV) back bone. Such group act as an anion receptor due to the electrophilicity of the aldehyde group. The hydroxyl which is an electron donating group can transfer the electron to the aldehyde group via the  $\pi$ -conjugated system of benzene ring to create an Internal charge transfer (ICT) which in turn reduce the radiative decay from the locally excited state and its emission. Structurally, PPE I is a homo-polymer which contain salicylaldehyde ethynylene as a repeating unit while PPE II possess an extra octoxyl substituent on the para position of the aromatic ring for solubility enhancement. On the other hand, PPE III and PPE IV are a random copolymer, and alternate copolymer, respectively. Both PPE III and PPE IV have an extra dibutoxyl-phenyleneethynylene for not only increase but also the spacer increase the solubility of these PPE as well between the salicylaldehyde receptor.



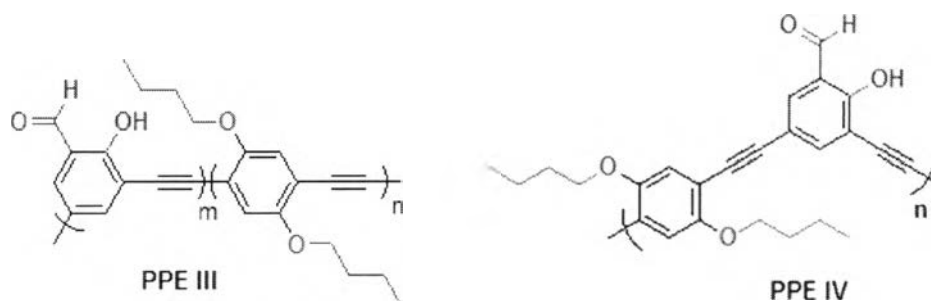
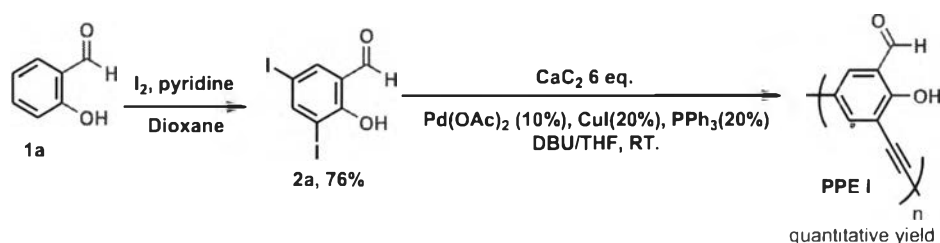


Figure 3.1 Structure of polymers PPE-I, PPE-II, PPE-III, and PPE-IV

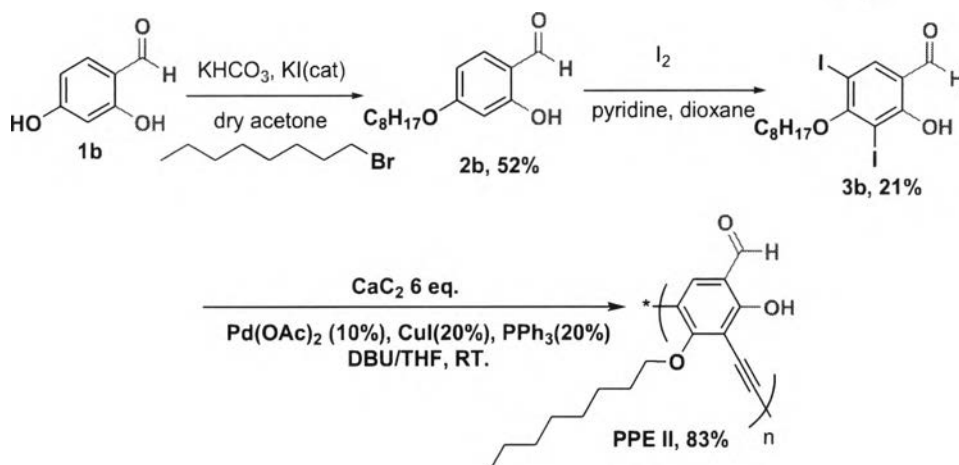
### 3.1.1 Synthesis and characterization of PPE I, and PPE II

Poly(phenylene ethynylene) (PPE I and PPE II) were synthesized via Sonogashira coupling reaction (Scheme 3.1). Salicylaldehyde (**1a**) was iodinated by the treatment of iodine in pyridine and 1,4-dioxane to afford 3,5-diiodosalicylaldehyde (**2a**) in 76% yield. Next, 4-hydroxysalicylaldehyde (**1b**) was prepared via alkylation reaction of **1b** with bromooctane using potassium bicarbonate and potassium iodide as a base and catalyst, respectively, in dry acetone to give the desired product **2b** in 52% yield. Next, 4-octylsalicylaldehyde (**2b**) was by using the same condition describe above to afford 3,5-diiodo-4-octylsalicylaldehyde (**3b**) in 21% yield. With the diiodo product **2a** and **3b** in hands, the PPEs containing salicylaldehyde (PPE I, and PPE II) directly from calcium carbide. Both PPE I and PPE II were prepared via Pd-catalyst cross coupling reaction by using calcium carbide reacting with 3,5-diiodosalicylaldehyde (**2a**) for PPE I and calcium carbide reacts with 4-octyl-3,5-diiodosalicylaldehyde (**3b**) for PPE II to get quantitative yield and 73% yields, respectively.



Scheme 3.1 Synthetic route of poly(phenylene ethynylene) PPE I





Scheme 3.2 Synthetic route of Poly(phenylene ethynylene) PPE I, and PPE II

For the NMR characterization,  $^1\text{H}$  NMR spectra of 3,5-diiodosalicylaldehyde (**2a**) are shown in Figure 3.2. All signals of 3,5-diiodosalicylaldehyde (**2a**) showed four singlet signals at 11.639, 9.664, 8.158 and 7.78 ppm corresponding to its aldehyde, hydroxyl, and aromatic proton, respectively.

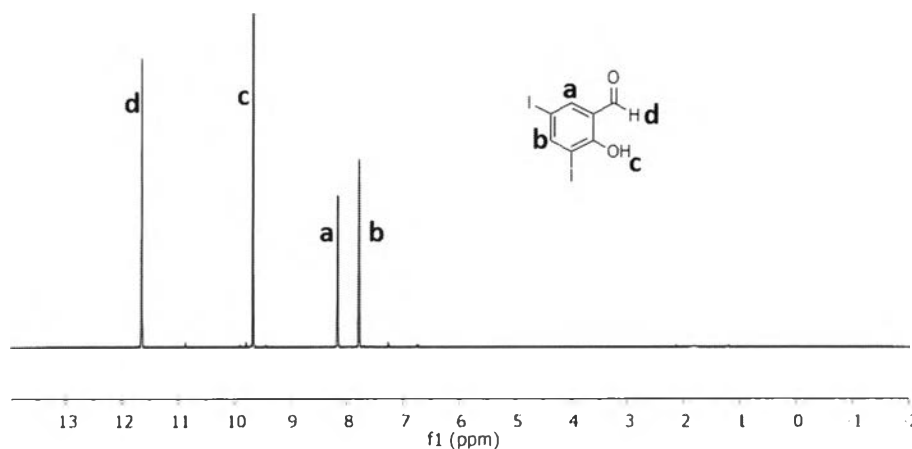


Figure 3.2  $^1\text{H}$  NMR of 3, 5-diiodosalicylaldehyde (**2a**)

The  $^1\text{H}$  NMR spectra of intermediate for PPE II (**2b**) and (**3b**) are shown in Figure 3.3. The starting material **2b** shown three singlets and two doublet signals at 11.47, 9.68, 7.39, 6.51 and 6.39 ppm which are corresponding to aldehyde, hydroxyl, and

aromatic proton. Moreover, the alkyl proton signal found at 0.86 to 4.00 ppm. Then, starting material **2b** have the iodination substitution on aromatic ring system, lose the two aromatic proton d, and e signal. In addition, aldehyde and hydroxyl proton found singlet at 12.02, and 9.67 ppm, which is down field than starting material **2b** and the CH<sub>2</sub> signal of octoxyl substitution on aromatic ring were detect at 4.03-0.94 ppm.

Moreover, we further characterized **PPE I** and **PPE II** by using FT-IR. Both of them shown O-H peak (O-H stretching) at 3397 to 3250 cm<sup>-1</sup> and carbonyl group at 1620 cm<sup>-1</sup> (**PPE I**) and 1721 cm<sup>-1</sup> (**PPE II**). The carbonyl peak in **PPE I** and **PPE II** shown lower energy than carbonyl in small molecule cause carbonyl in this case can be conjugate with polymer backbone and it can generate interaction or H-bonding between aldehyde and hydroxyl group (**Figure 3.3** and **3.4**). However, the FT-IR results revealed that **PPE II** have impurity in the polymer because low intensity spectrum of aldehyde and carbonyl peak.

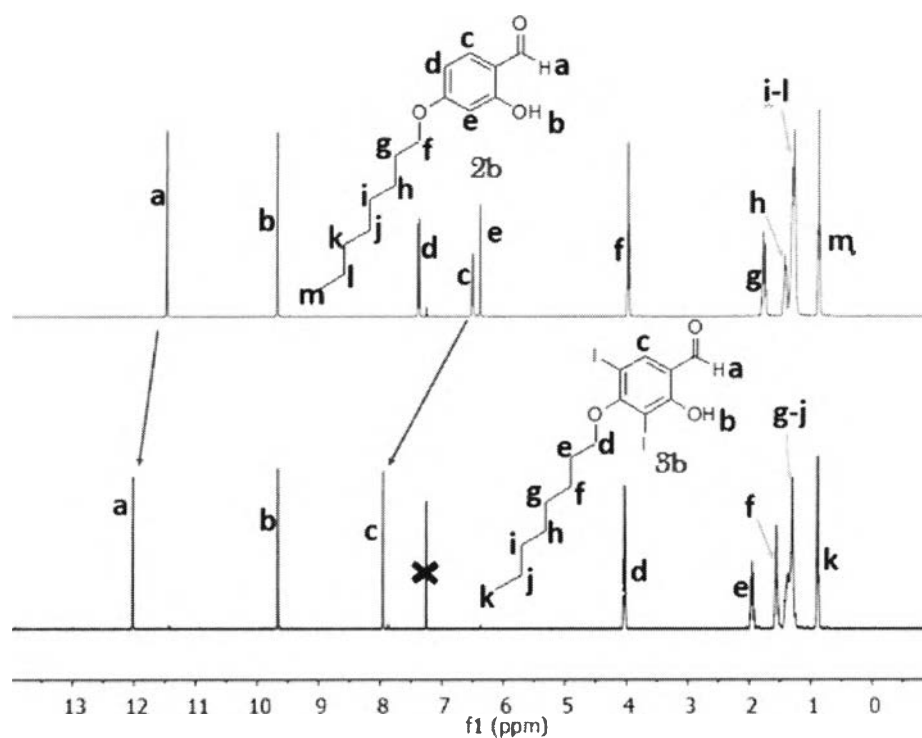


Figure 3.3 <sup>1</sup>H NMR of **2b** and **3b**

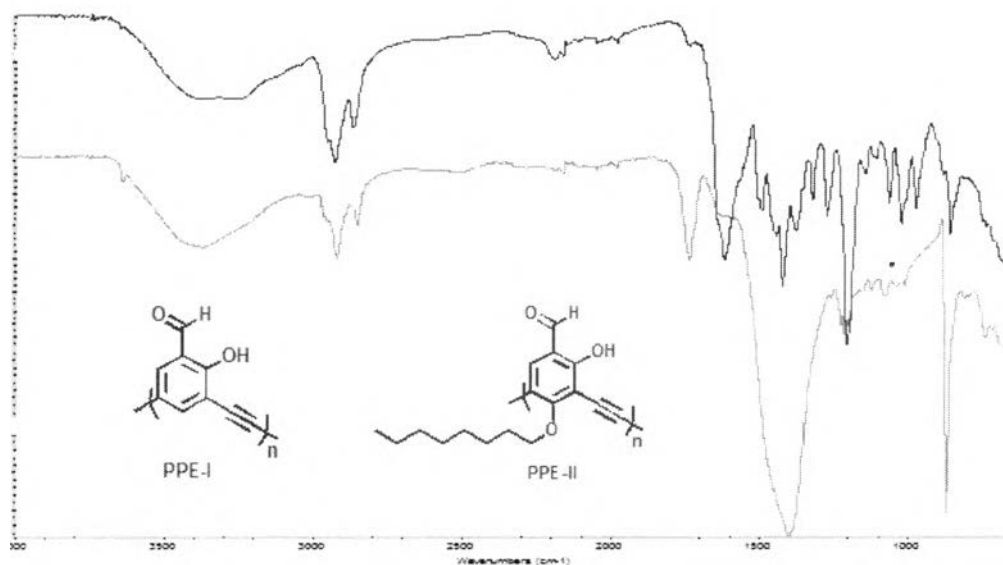
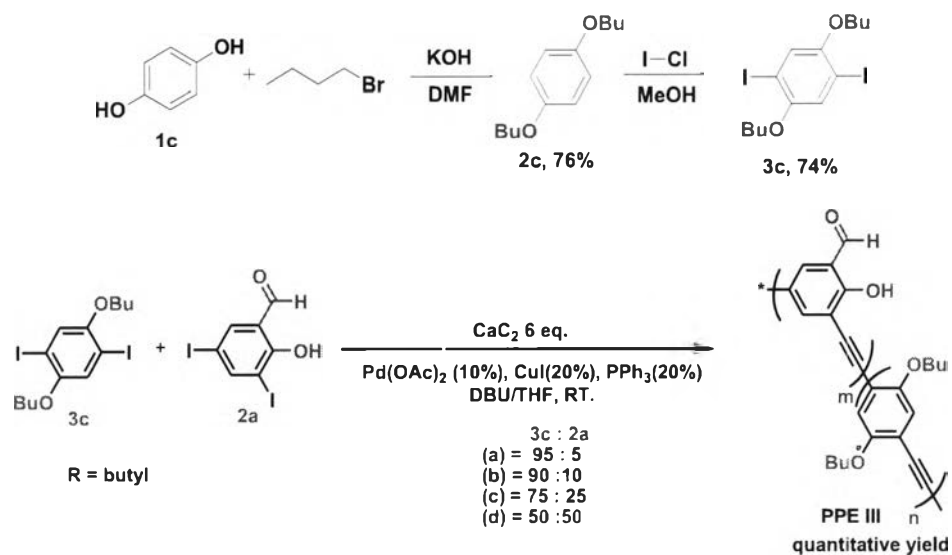


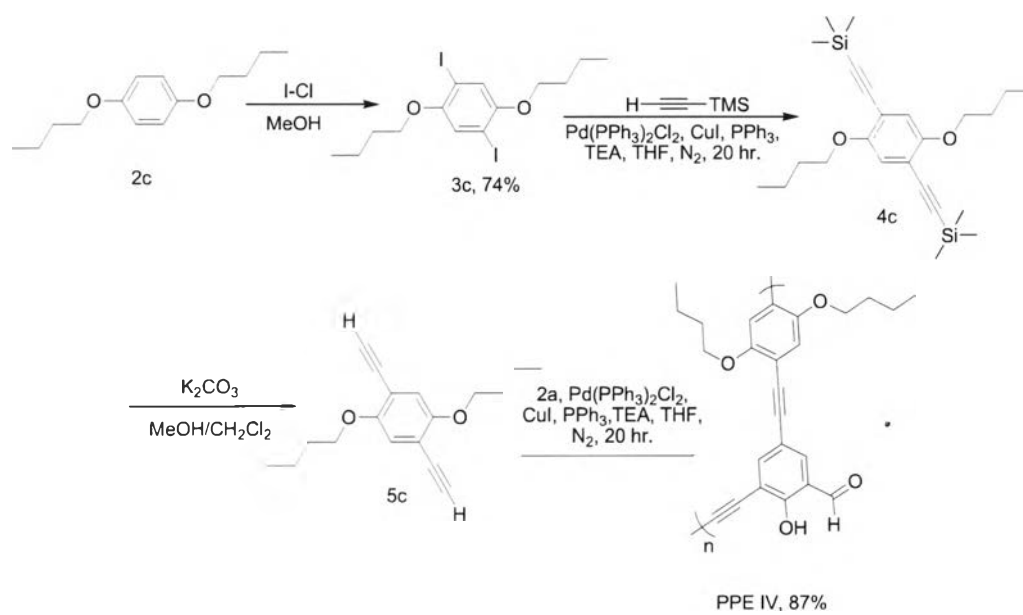
Figure 3.4 FT-IR spectrum of PPE I and PPE II

### 3.1.2 Synthesis and characterization of PPE III, and PPE IV

1,4-dibutoxy-2,5-diiodobenzene (**3c**) was synthesized by alkylation of hydroquinone (**1c**) using potassium hydroxide in DMF, followed by iodination in iodine monochloride in MeOH to give the target monomer **3c** in 74 % yield as shown in **Scheme 3.3**. As described above that PPE III is the random copolymer which are design for increase the solubility, therefore Pd-catalyst cross coupling reaction by using calcium carbide with 3,5-diiodosalicylaldehyde (**2a**) and dibutoxy-diiodobenzene (**3c**) in various ratio (95%, 90%, 75%, and 50% as show in **Scheme 3.3**. All the resulting polymer afford in quantitative yields. On the other hands, the synthesis of PPE IV which is the alternate copolymer began with Sonogashira coupling of 1,4-dibutoxy-2,5-diiodobenzene (**3c**) with TMS-acetylene to afford compound **4c**. Then desilylation of compound **4c** with  $K_2CO_3$  in MeOH/ $CH_2Cl_2$  to afford compound **5c**. Finally, PPE IV was synthesized via Sonogashira cross coupling between 3,5-diiodosalicylaldehyde (**2a**) and 2,5-dibutoxy-1,4-ethynylacetylene (**5c**) using TEA base in THF to afford produce PPE IV in 73 % yield (**Scheme 3.4**).



Scheme 3.3 Synthetic route of Poly(phenylene ethynylene) PPE III

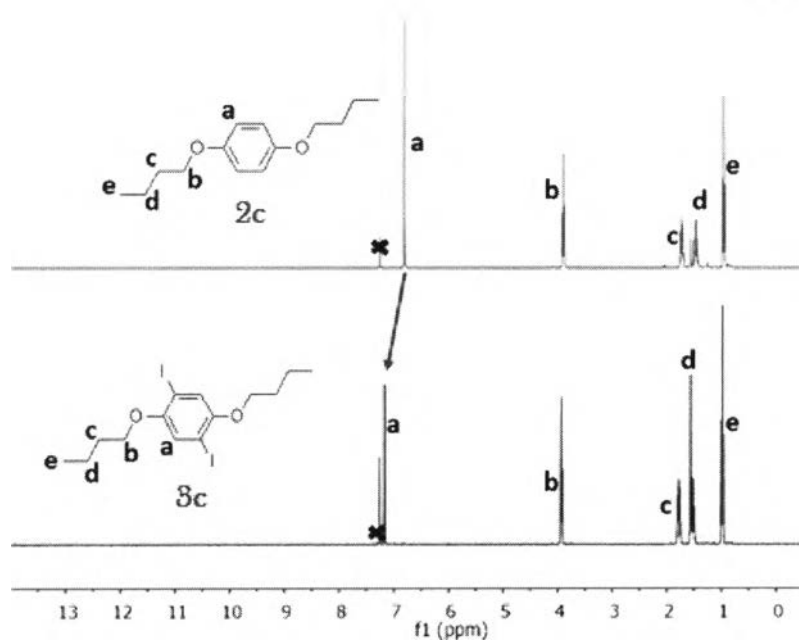


Scheme 3.4 Synthetic route of Poly(phenylene ethynylene) PPE IV



1729542247

The  $^1\text{H}$  NMR of **2c** and **3c** are shown in **Figure 3.5**. The compound **2c** showed one singlet peak at 6.82 ppm corresponding to an aromatic proton and two peaks around 0.97 to 3.91 ppm belonging to  $\text{CH}_2$  on butoxyl group. After iodination of **2c** the aromatic proton at position **a** of product **3c** was located down field than the aromatic proton on starting material due to successful iodine substitution. In addition, the  $^1\text{H}$  NMR of monomer compound **4c**, and **5c** are shown in **Figure 3.6**. The extra signal of **4c** at 0.97 ppm belongs to the trimethyl silyl group, confirming successful Sonogashira coupling reaction of **3c** with TMS-acetylene. The desilylation of **4c** to compound **5c** was confirmed by the disappearance of TMS proton at 0.97 ppm and the new singlet proton at 3.33 ppm which belongs to terminal alkyne proton.



**Figure 3.5**  $^1\text{H}$  NMR of 1,4-dibutoxybenzene (**2c**) and 2,5-dibutoxy-1,4-diiodobenzene (**3c**)

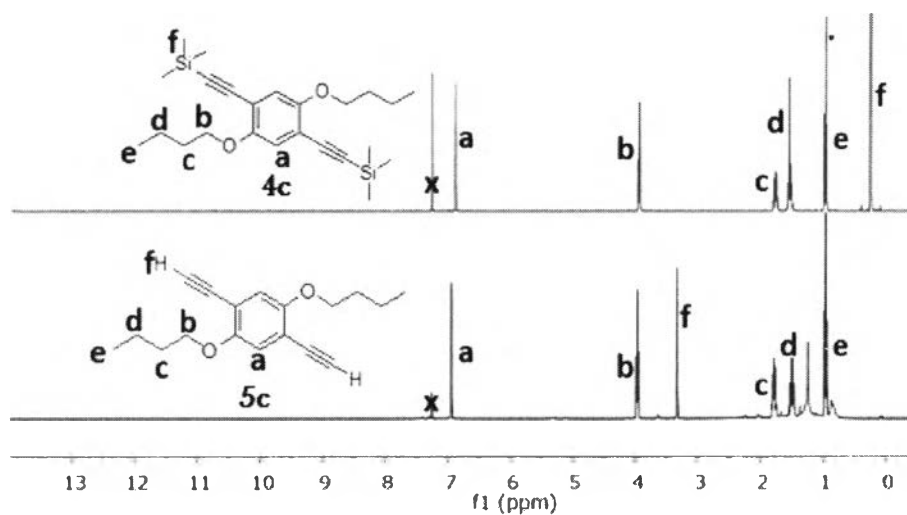


Figure 3.6  $^1\text{H}$  NMR of 4c, and 5c

The FT-IR characterization of PPE III were compare with poly(phenylene ethynylene) PPE-z which have no salicylaldehyde unit (in Figure 3.8). From the FT-IR results shown O-H peak at  $3300\text{-}3200\text{ cm}^{-1}$ , and carbonyl peak at  $1621\text{ cm}^{-1}$  in case of PPE III while the PPE-z does not show the aforementioned peak. This results confirm the formation of PPE III containing both salicylaldehyde and dibutoxy moiety as random copolymer. PPE IV also shown O-H, aldehyde, and carbonyl peak as the same position with PPE III (Figure 3.7).



1729542247



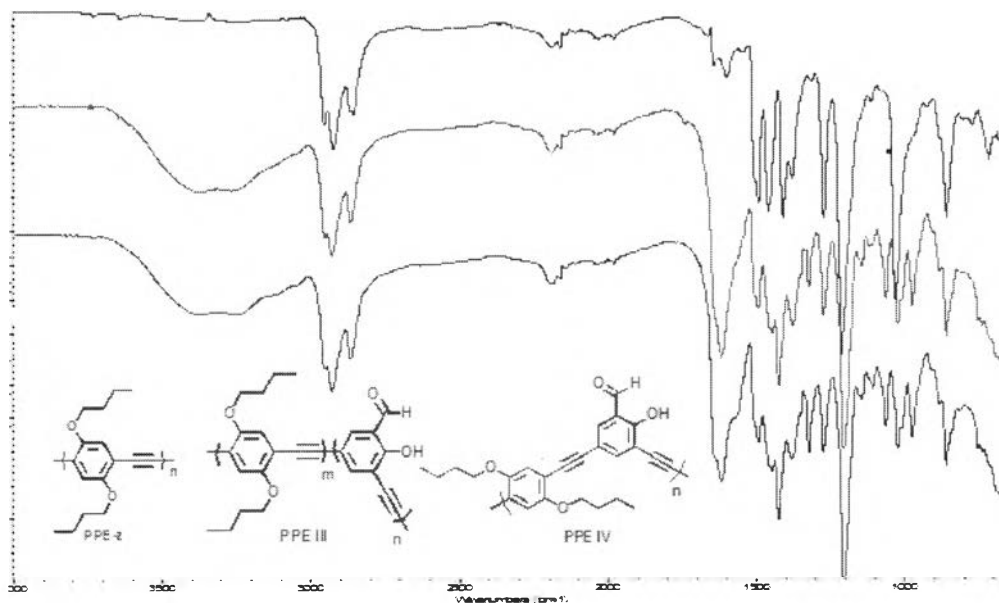


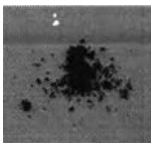

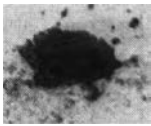

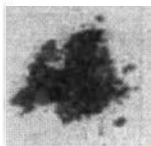

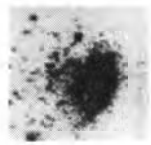
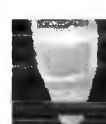

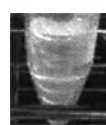
Figure 3.7 FT-IR spectrum of PPE III (red spectrum) compare with poly(phenylene ethynylene) (blue spectrum) which is no element of salicylaldehyde unit

### 3.1.3 Molecular weight determination and photophysical properties of PPEs

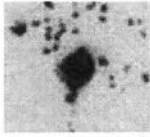
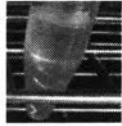
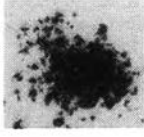
The appearance, molecular weight and solubility of all synthesized polymers were summarized in **Table 3.1**. For the solubility, **PPE I** and **PPE II**, were not soluble in any organic solvent but partially soluble in THF in case of **PPE II**. On the other hands **PPE III (a-d)** and **PPE IV** were soluble in various organic solvents such as THF, methylene chloride, and chloroform. This is caused by the addition alkoxy part in the polymer which increases their solubility. Later, all the **PPEs** molecular weights were determined by GPC using polystyrene as standard. The molecular weight of **PPE II** is  $9.5 \times 10^3$  when determined from the soluble part in THF but **molecular weight of PPE I** cannot be determined due to its poor solubility. Additionally, **PPE III (a-d)** and **PPE IV** were completely dissolved in THF and molecular weights were found in the range of  $9.5 \times 10^3$  to  $1.86 \times 10^4$  (**Table 3.1**). The fluorescence emission under black light was depicted in **Table 3.1** (last roll). Poor fluorescence intensity were found in case of homo polymer **PPE I** and **II** as green and blue color. In case of random copolymer **PPE III**, we found that an increase in diiodosalicylaldehyde co-monomer ratio leads to

a reduction in emission intensity under backlight. This behavior is caused by the ICT effect governed by the salicylaldehyde group. This result indicates that the intensity of fluorescence is dependent on the salicylaldehyde group, which cooperated in the polymer backbone. The presence of these groups lowers the emission intensity under back light in our prepared PPEs in comparison to conventional PPEs. Thus, our PPEs are suitably designed as a fluorescence turn on chemosensor.

**Table 3.1** Molecular weight, solubility, characteristics of polymer, and color under backlight of all PPEs.

Type of PPEs	Molecular weight (Da)	Solubility in THF	Characteristics of polymers	Color under backlight
PPE I	-	None		
PPE II	$9.5 \times 10^3$	Poor		
PPE III(a)	$1.86 \times 10^4$	Good		
PPE III(b)	$1.85 \times 10^4$	Good		
PPE III(c)	$9.5 \times 10^4$	Good		



PPE III(d)	$1.51 \times 10^4$	Good		
PPE IV	$6.5 \times 10^3$	Soluble		

### 3.1.4 Sensing ability of PPE I, PPE II, PPE III, and PPE IV

We begin our study of the sensing properties of PPE I and PPE II. As mentioned above, PPE I and II were poorly soluble in THF. The partial solution of PPE I and PPE II (unknown concentration) in THF were mixed with HEPES buffer solution in 9:1 ratio before being exposed to an excess amount of sodium cyanide (1 mM). We found that sodium cyanide solution increased the fluorescence emission signal of PPE I ( $I/I_0 = 9.69$ ) and PPE II ( $I/I_0 = 2.16$ ) (Figure 3.8). Even though PPE I and PPE II are poorly soluble in THF, the result of this preliminary analysis suggested that these PPEs have good potential as a fluorescence cyanide detector.

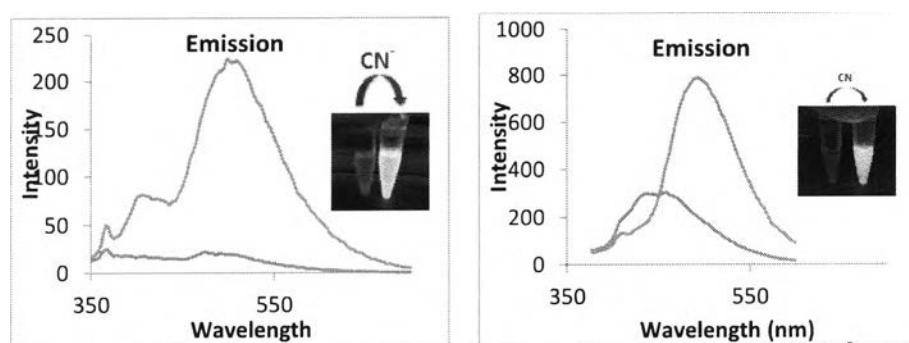
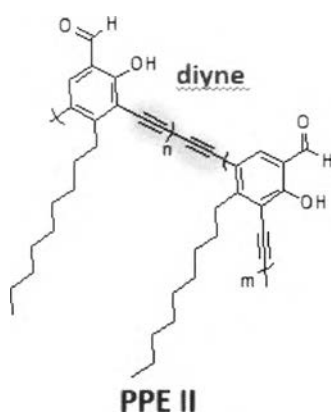


Figure 3.8 Emission spectra of the solution of PPE I and PPE II upon the addition of sodium cyanide (1 mM) in 90% THF/10 mM HEPES buffer pH 7.4 ( $\lambda_{\text{ex}} = 341$  nm (PPE I) and  $\lambda_{\text{ex}} = 365$  nm (PPE II))

In order to quantify the sensitivity and selectivity, we next focused on the sensing ability of PPE II due to their partial solubility in THF. At 50  $\mu\text{M}$  concentration of PPE II, it was tested with cyanide ion and other anions at 10 equivalents (500  $\mu\text{M}$ ) such as  $\text{F}^-$ ,  $\text{I}^-$ ,  $\text{Cl}^-$ ,  $\text{Br}^-$ ,  $\text{OAc}^-$ ,  $\text{SO}_3^{2-}$ ,  $\text{NO}_3^-$ ,  $\text{HCO}_3^-$ ,  $\text{NO}_2^-$ ,  $\text{SCN}^-$ ,  $\text{SO}_4^{2-}$ , and  $\text{N}_3^-$  as shown in **Figure 3.10** (left-hand column). Unfortunately, the fluorescence emission intensity of all tested anions remained unchanged. When the concentration of fluorophore PPE II were increased to 100  $\mu\text{M}$ , the intensity of fluorescence emission toward cyanide anion (1000  $\mu\text{M}$ ) only increased slightly while the response to other anion remained unchanged as shown in **Figure 3.10** (right hand column). We believe that poor sensitivity of PPE towards cyanide ions is due to the poor polymerization causing polymer defection. The defection of polymer can be confirmed by FT-IT spectrum as seen in **Figure 3.4** that has less intensity of carbonyl peak around  $1700\text{ cm}^{-1}$  as mentioned above.

Based on the results above, we conclude that PPE I and PPE II cannot be used as a cyanide ions sensor because of a solubility problem and the problem of polymer defection during polymerization. We hypothesize that the formation of diyne moiety occurs causing a polymer defect as shown in (**Figure 3.9**). This disturbs the conjugate back bone and lowers the conjugate length of resulting polymers.



**Figure 3.9** The polymer defection caused by the diyne unit

In addition, the PPE III and PPE IV copolymer were tested for sensing activity with cyanide ions and other anions. However, the PPE III (c) and PPE IV fluorescent signal were not responsive to any anions at 100  $\mu\text{M}$  concentration (**Figure 3.11**). This

is perhaps caused by the present of dibutoxy arene as a component in our molecule resulting in high basal fluorescent intensity prior to the addition of cyanide anion (Table 1). Moreover, poor polymerization as shown in low molecular weight of resulting polymers (table 3.1), suggest that polymer defect may have occurred. Thus, the fluorescence enhancement of PPE III and PPE IV could not be achieved.

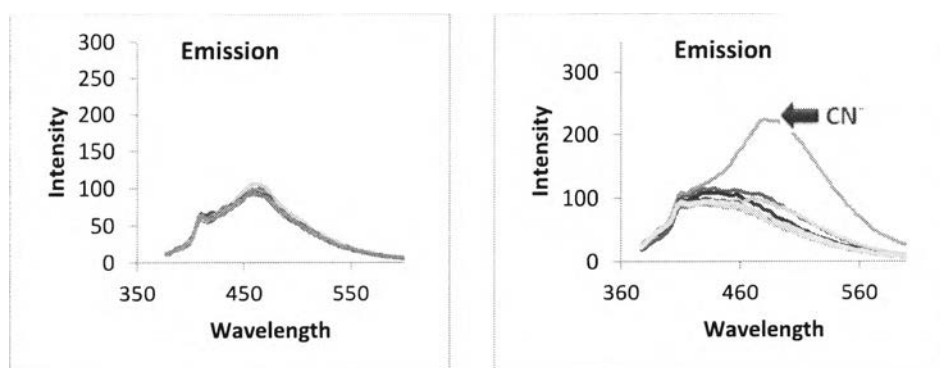


Figure 3.10 PPE II 50  $\mu\text{M}$  (left) and 100 $\mu\text{M}$  (right) upon the addition of NaCN and other anions 10 eq. ( $\lambda_{\text{ex}} = 365 \text{ nm}$ )

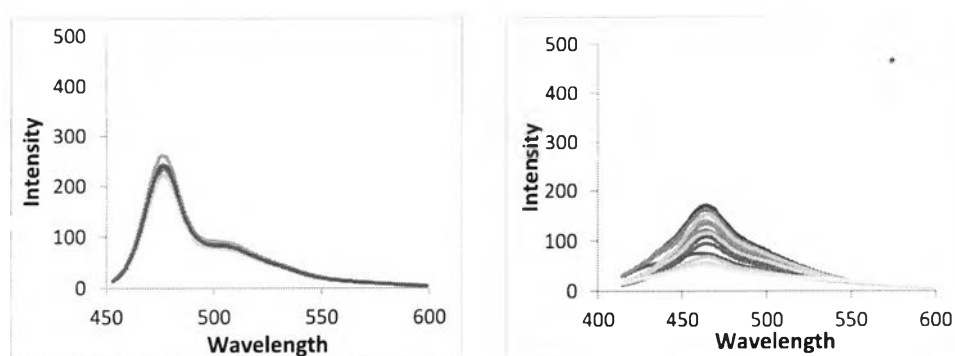
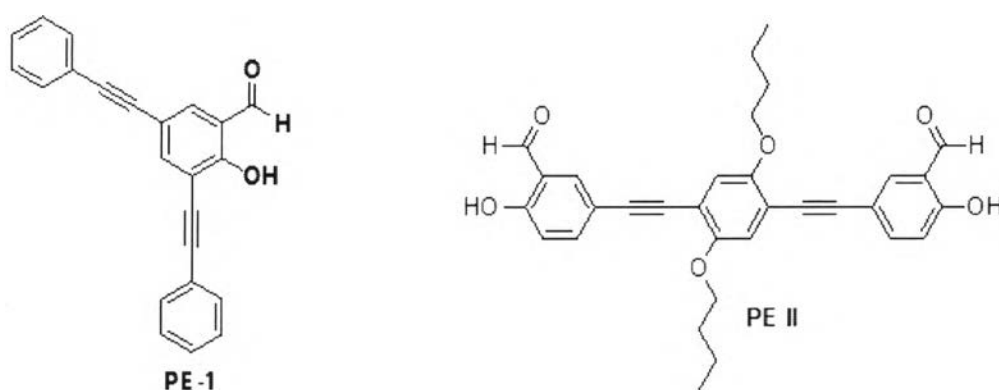


Figure 3.11 PPE III (left) and PPE IV (right) 10 $\mu\text{M}$  upon the addition of NaCN and other anion (10 eq.) in 90% THF/10 mM HEPES buffer pH 7.4 ( $\lambda_{\text{ex}} = 417 \text{ nm}$ ,  $\lambda_{\text{em}} = 463 \text{ nm}$ )

Based on the results above, we conclude that four prepared polymers (PPE I, PPE II, PPE III, and PPE IV) cannot be used as a sensor for the detection of cyanide ions. To overcome aforementioned problems, we subsequently synthesized small molecules containing phenylene ethynylene group as a signaling unit and salicylaldehyde group as a sensory unit as described in the next section.

### 3.2 Cyanide fluorescence sensors from PE I and PE II

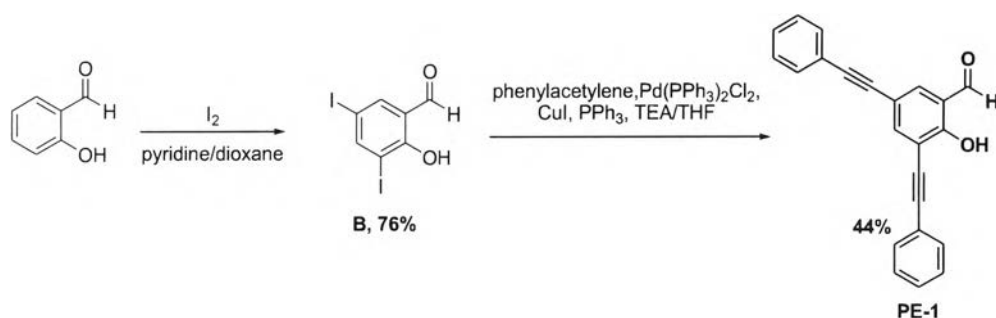
As mentioned above, in this section we turn our attention to small molecule composed of phenylene ethynylene (PE) unit as a molecular sensor. In this section, we designed and synthesized phenyleneethynylene fluorophores PE I and PE II as shown in **Figure 3.12**. Similarly, PE I and PE II contain the same signaling unit which comprises of two phenylene ethynylene groups. However, they differ in their sensing unit. PE I possess one salicylaldehyde group while PE II contains two salicylaldehyde groups. These differences were intentional as it allows us to compare their selectivity and sensitivity toward anions, especially cyanide.



**Figure 3.12** Structure of PE I and PE II

#### 3.2.1 Synthesis and characterization of PE I and PE II

Initially, fluorophore PE I was synthesized according to **Scheme 3.4** using Sonogashira cross coupling reaction as a key step. 3,5-diiodosalicylaldehyde **2a** were reacted with phenylacetylene via Sonogashira coupling using TEA in THF as solvent to give PE I in 44% (**Scheme 3.5**)



Scheme 3.5 Synthetic route of phenylene ethynylene PE I

$^1H$  NMR spectra of compound **2a** and PE I are shown in Figure 3.13. All signals can be assigned to all protons in each corresponding structure. **2a** showed four singlet signals at 11.63, 9.66, 8.15, and 7.77 ppm corresponding to its aldehyde, hydroxyl, and aromatic protons, respectively. For the PE I, the aldehyde product showed more up field pattern in general in comparison with starting material at **2a** ppm. The multiplet signal at 7.34-7.88 ppm belongs to aromatic proton from phenylacetylene, confirming a successful coupling reaction.

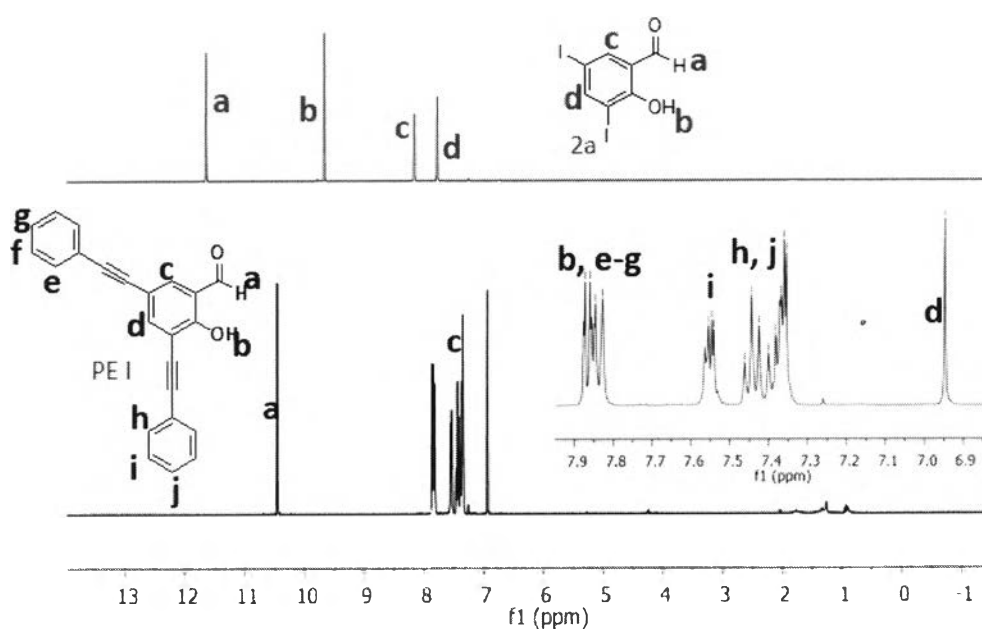
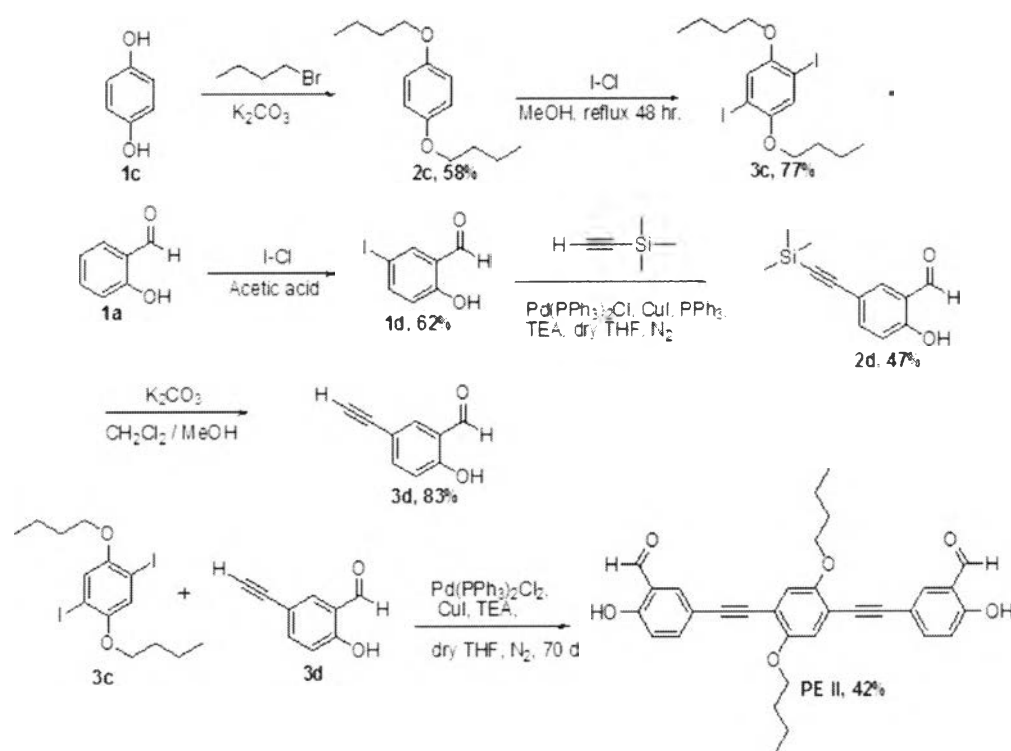


Figure 3. 13  $^1H$  NMR (400 MHz) spectra of starting material compound B and PE I

On the other hands, the fluorophore PE II was synthesis according to Scheme 3.5. The first diiodo coupling partner 2,4-dibutoxy-1,2-diiodobenzene (**3c**) were synthesized by alkylation of hydroquinone (**1c**) with bromobutane using  $K_2CO_3$  in acetonitrile, followed by iodination to afford target **3c**. For the second coupling partner, diyne **3d**, we began with iodination of salicylaldehyde (**1a**) with iodine-monochloride in methanol and followed by Sonogashira coupling with protected acetylene to afford compound **2d** in 30 % for two step reaction. Then desilylation of compound **2d** with  $K_2CO_3$  in MeOH/ $CH_2Cl_2$  afford target compound **3d** in 83% yield. With the two coupling partners **3c** and **3d** in hands, PE II was successfully synthesized by Sonogashira coupling reaction between **3d** and **3c** using TEA base in THF to afford PE II in 42% yield.



Scheme 3.5 Synthetic route of phenylene ethynylene PE II

The  $^1H$  NMR spectra of compound **3d**, **3c**, and PE II are shown in Figure 3.14. The starting material **3d** showed important signals at 11.13, 9.87 and 3.04 ppm corresponding to aldehyde (i), hydroxyl (j), and terminal alkyne (k). The double coupling reaction between **3c** with **3d** leading to PE II were accomplished confirming



by the presence of singlet aldehyde peak (i) and hydroxyl peak (j) at 11.13 and 9.89 ppm as well as the signals of butoxy group (a-e) at 4.04, 1.85, 1.56, and 1.01 ppm

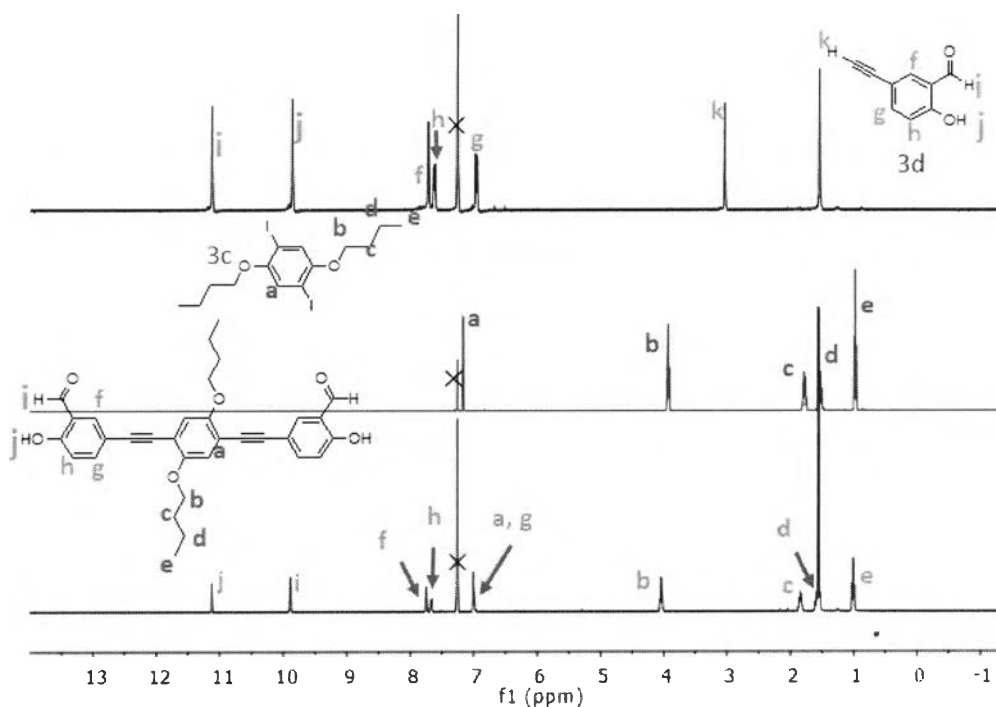
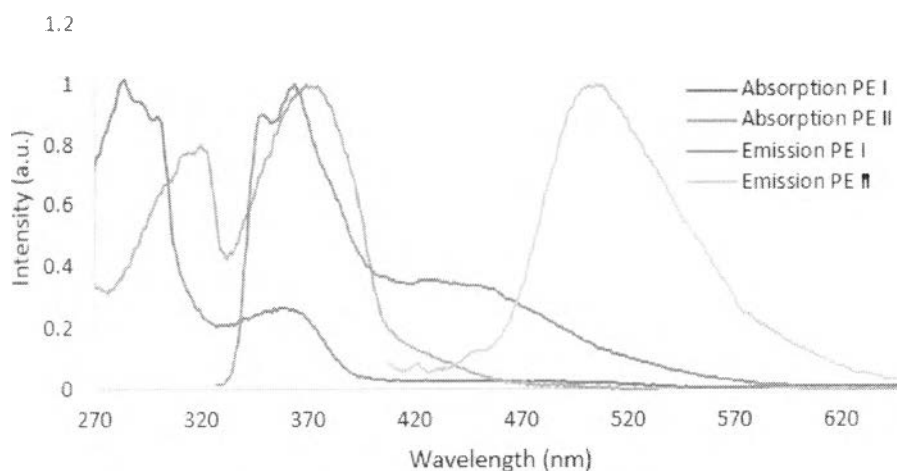


Figure 3.14  $^1\text{H}$  NMR (400 MHz) spectra of **3d**, **3c**, and PE II

### 3.2.2 Photophysical properties study of PE I and PE II

The absorption and emission spectroscopy of PE I and PE II were studied in an aqueous DMSO solvent and their photophysical properties are shown in **Table 3.2**. The fluorophore exhibited two major absorption maxima around 301 for PE I and 369 nm for PE II (**Figure 3.18**). These absorbance are associated with two  $\pi\text{-}\pi^*$  electron transition ( $S_0 \rightarrow S_2$  and  $S_0 \rightarrow S_1$ ) of the  $\pi$ -conjugated phenylene ethynylene system [43]. PE I and PE II fluorophore showed a singlet maximum emission wavelength around 363 and 504 nm respectively (**Figure 3.15**). The greater stroke shift of PE II implied greater involvement of the ICT process in the excited state of their fluorophore.



**Figure 3.15** Normalized absorption spectra PE I and PE II (10  $\mu\text{M}$ ) in 90%DMSO/10 mM HEPES buffer pH 7.4

**Table 3.2** Photophysical properties of PE I and PE II

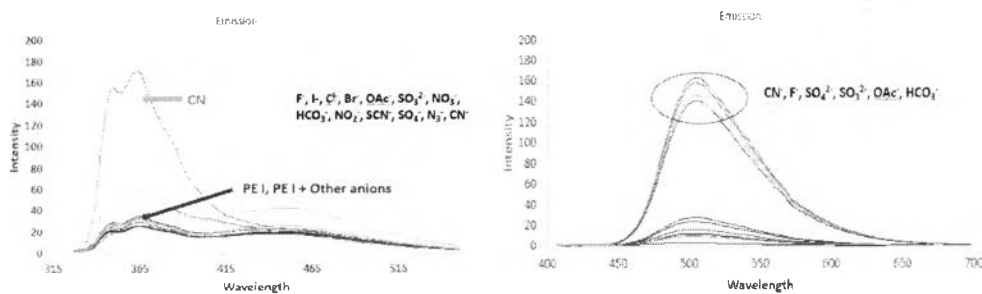
Compound	$\lambda_{\text{ab}}$ (nm)	$\log \epsilon$	$\lambda_{\text{em}}$ (nm)
PE I	301	5.347	363
PE II	369	5.006	504

\* Photophysical properties of PE I and PE II study in 90%DMSO/10  $\mu\text{M}$  HEPES buffer pH 7.4

### 3.2.3 Screening of PE I and PE II toward anions

In this section, we tested PE I and PE II with 12 different anions such as  $\text{F}^-$ ,  $\text{I}^-$ ,  $\text{Cl}^-$ ,  $\text{Br}^-$ ,  $\text{OAc}^-$ ,  $\text{SO}_3^{2-}$ ,  $\text{NO}_3^-$ ,  $\text{HCO}_3^-$ ,  $\text{NO}_2^-$ ,  $\text{SCN}^-$ ,  $\text{SO}_4^{2-}$ ,  $\text{N}_3^-$  and  $\text{CN}^-$  and the result were summarized in **Figure 3.16** (left) for PE I and **Figure 3.16** (right) for PE II. In case of PE I, the fluorescence emission increased ( $I/I_0 = 5.34$ ) upon the addition of cyanide anion at 10  $\mu\text{M}$  concentration while it remained unchanged in the presence of 11 other anions (**Figure 3.16** left). This showed a promising result for cyanine sensing

application. On the other hands, **PE II** displayed a lower selectivity and sensitivity toward tested anions. At the concentration of anion at 150  $\mu\text{M}$ , the fluorescence emission in case of  $\text{F}^-$ ,  $\text{OAc}^-$ ,  $\text{SO}_3^{2-}$ ,  $\text{HCO}_3^-$ , and  $\text{CN}^-$  were enhanced while there were insignificant change in response to other anions (**Figure 3.16 right**). It is worth noting that even though **PE II** demonstrated low selectivity toward a panel of anion, the fact that it response well to fluoride ion suggest that it could be a promising sensor for fluoride.

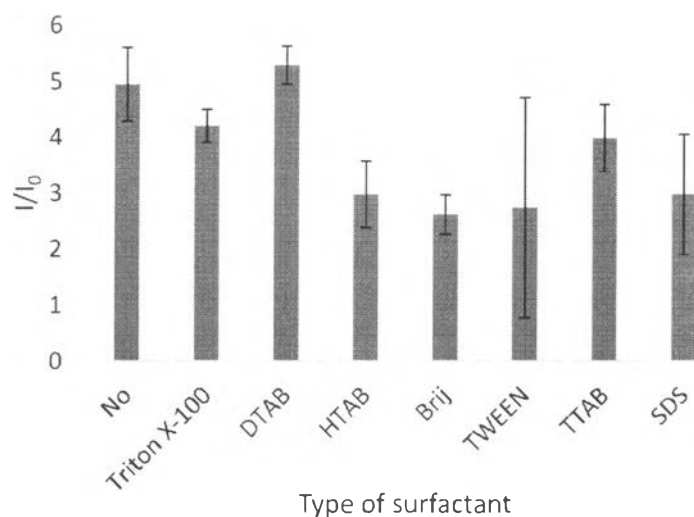


**Figure 3.16** Emission spectrum of **PE I** (left) and **PE II** (right) at 5  $\mu\text{M}$  with 13 anions 2 eq and 30 eq, respectively in 90% DMS in HEPES buffer pH 7.4

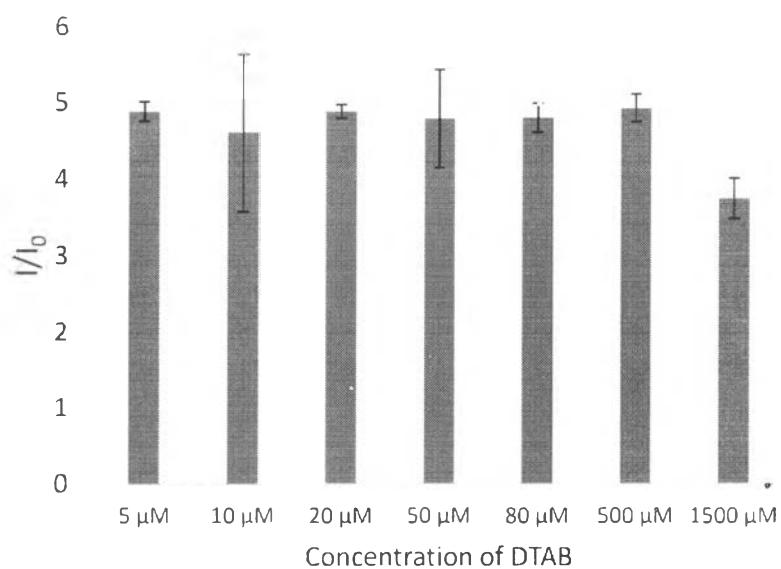
### 3.2.4 Fluorescence sensor study of PE I

From the screening results above, **PE I** was further investigated for cyanide ion sensing application in terms of sensitivity and selectivity. So, we began to study and optimize the condition to improve sensing ability of **PE I** for the detection of cyanide ion

Since the cyanide ( $\text{CN}^-$ ) anions are soluble in water, we performed the measurement in a mixed solvent of aqueous DMSO and HEPES buffer pH 7.4. Since it is well known that surfactants could increase the fluorescence intensity of fluorophore by reduction of aggregation and also by reduction of non-specific interactions, we therefore studied the effect of surfactants to the sensing ability of **PE I** with cyanide anion. As depicted in (**Figure 3.17**), among all tested surfactants, the cationic surfactants (DTAB and TTAB) generally gave higher sensitivity than the anionic surfactant such as SDS and nonionic surfactant such as Brij and TWEEN20. DTAB was therefore chosen in our case and we further investigated the effect of changing in concentration of such surfactants. We found that the concentration of DTAB did not affect sensitivity of **PE I** towards cyanide anion (**Figure 3.18**)



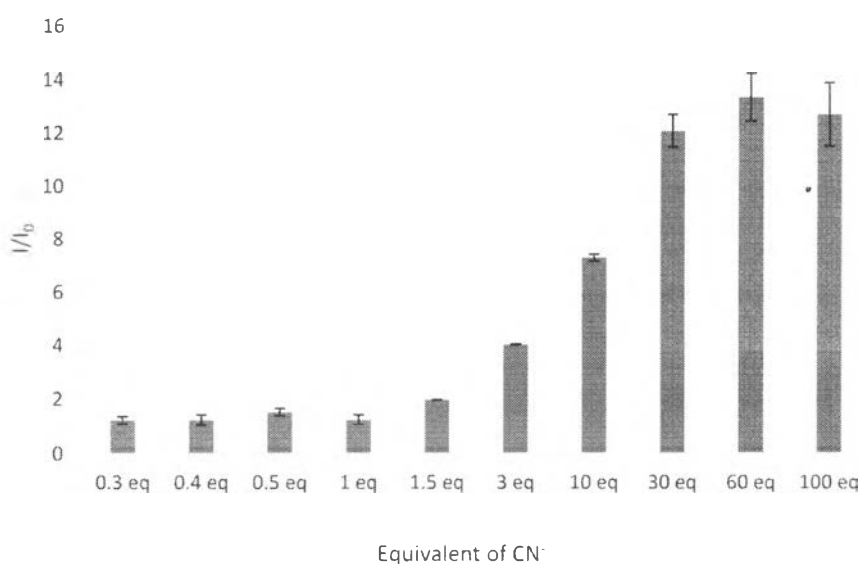
**Figure 3.17** Bar chart representing the fluorescence enhancement ( $I/I_0$ ) of PE I ( $5 \mu\text{M}$ ) upon the addition of sodium cyanide (2 eq) in HEPES buffer pH 7.4 (10 mM) in the presence of various surfactants (10 mM). The fluorescence intensity at the emission peak of each system was used.



**Figure 3.18** Bar chart representing the fluorescence enhancement ( $I/I_0$ ) of PE I ( $5 \mu\text{M}$ ) upon the addition of sodium cyanide (2 eq) in HEPES buffer pH 7.4 (10 mM) in the presence of various surfactants (10 mM). The fluorescence intensity at the emission peak of each system was used.

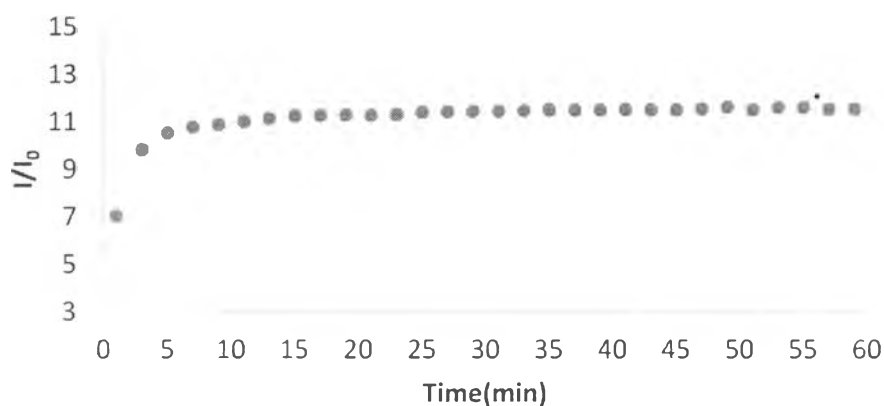


With the optimized condition in hands, the fluorescence intensity in relation to cyanide concentration was investigated upon the addition of various equivalent of sodium cyanide in an aqueous solvent (HEPES buffer pH 7.4, 20  $\mu\text{M}$  DTAB). The fluorescence intensity initially increased almost linearly with the cyanide concentration up to 30 equivalent (150  $\mu\text{M}$ ) (Figure 3.19). It is important to mention that the emission spectra were acquired at 30 minute for all sensing experiment to ascertain the completion within 6 minute of the reaction.



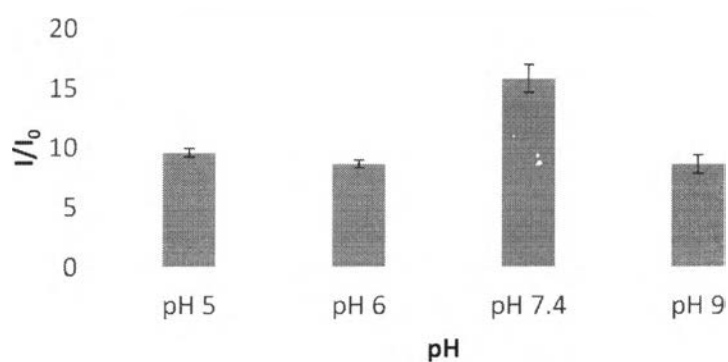
**Figure 3.19** The bars represent the fluorescence enhancement ratio ( $I/I_0$ ) of PE I (5  $\mu\text{M}$ ) at various equiv of cyanide in DTAB (20 mM)/HEPES buffer pH 7.4 (10mM).

Next, as we realized that this fluorescence of PE I toward cyanide is an reaction mode which is time dependent and 30 minute prior the measurement might not be enough to get the highest signal enlargement. We therefore study effect of reaction time with the fluorescence intensity of PE I with cyanide anioin (Figure 3.20). It shown that the fluorescence enhancement ratio were exponentially increased to 5 min and stable after that. Therefore the 6 minutes measurement time were selected as optimal time.



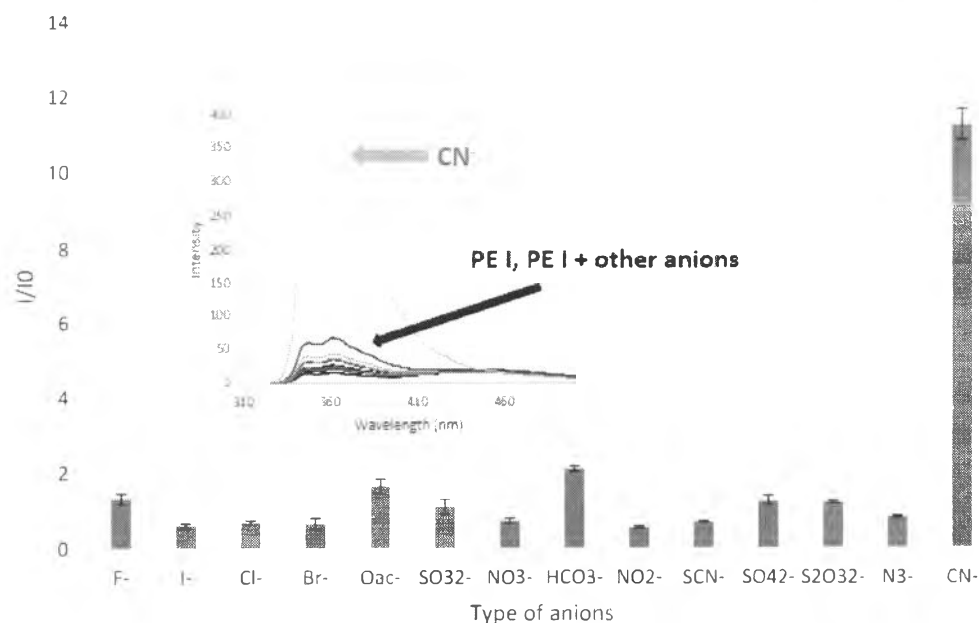
**Figure 3.20** Time-dependent changes in the fluorescence intensity of PE I ( $5\mu\text{M}$ ) upon addition of cyanide 30 equivalent in DTAB (20 mM)/HEPES buffer pH 7.4 (10mM).

The next parameter investigated was the pH. The pH variation were varied in the range of 5-9 (pH 5, 6, 7.4, and 9) and the fluorescence enhancement ratio of PE I toward cyanide were monitored (**Figure 3.21**). The pH also showed only little effect of the pH in the range of 5-9 as fluorescence enhancement ratio were found in the range between 8 -12. However the best condition is the pH at 7.4 which is also suitable for use this sensor in the physiology condition for the cyanide detection.



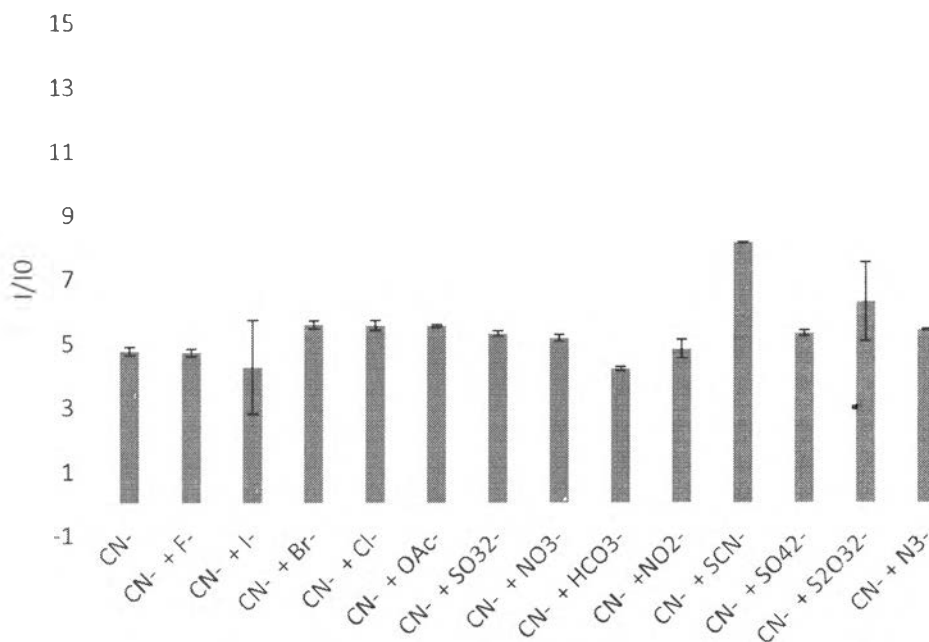
**Figure 3.21** Bar represent the fluorescence enhancement ratio ( $I/I_0$ ) of PE II ( $5\mu\text{M}$ ) at various pH of buffer ( $10\mu\text{M}$  in DTAB ( $20\mu\text{M}$ ) upon the addition of CN- 60 equiv.

With the optimized condition in hand, we retested the PE I toward cyanide and other anion again using the optimal condition. The results were present in **Figure 3.22**. Upon the addition of cyanide anion at 150  $\mu\text{M}$  concentration, the fluorescence enhancement ratio were found ca. 11.77 while the other anion remain almost unchanged at less than 2.



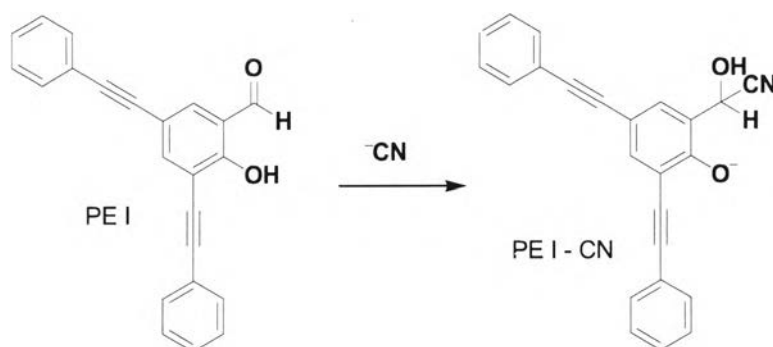
**Figure 3.22** Fluorescence enhancement ratio ( $I/I_0$ ) of PE I in the presence of various anions. The data were based on the fluorescence intensity at 363 nm acquire from the solution in 10  $\mu\text{M}$  HEPES buffer pH 7.4 containing DTAB 20  $\mu\text{M}$  with PE I 5  $\mu\text{M}$  and anions 30 eq.

For the interference test, we the selectivity test of PE I found that it can exhibited high specific toward cyanide ion (**Figure 3.23**). In the other hand, interference test found that SCN<sup>-</sup> are increasing fluorescence signal of PE I toward CN<sup>-</sup> (**Figure 3.23**).



**Figure 3.23** Fluorescence enhancement ratio ( $I/I_0$ ) of PE I in the presence of cyanide ion and another anion. The data were based on the fluorescence intensity at 363 nm acquire from the solution in 10  $\mu\text{M}$  HEPES buffer pH 7.4 containing DTAB 20  $\mu\text{M}$  with PE I 5  $\mu\text{M}$  and anions 0.15 mM.

Finally,  $^1\text{H-NMR}$  titration study of PE I in DMSO- $\text{D}_6$ , it found that when addition of sodium cyanide 0.8 – 2.4 equivalent the peak at 10.38 ppm were decrease continuously while peak at 8.5 ppm also were increase continuously (**Figure 3.24**). We belived that the new peak is belong to the H at the cyanohydrin intermediate (PE I – CN) resulting from to the attack of cyanide at aldehyde group (**Scheme 3.6**).



**Scheme 3.6** The mechanism of PE I toward cyanide ion



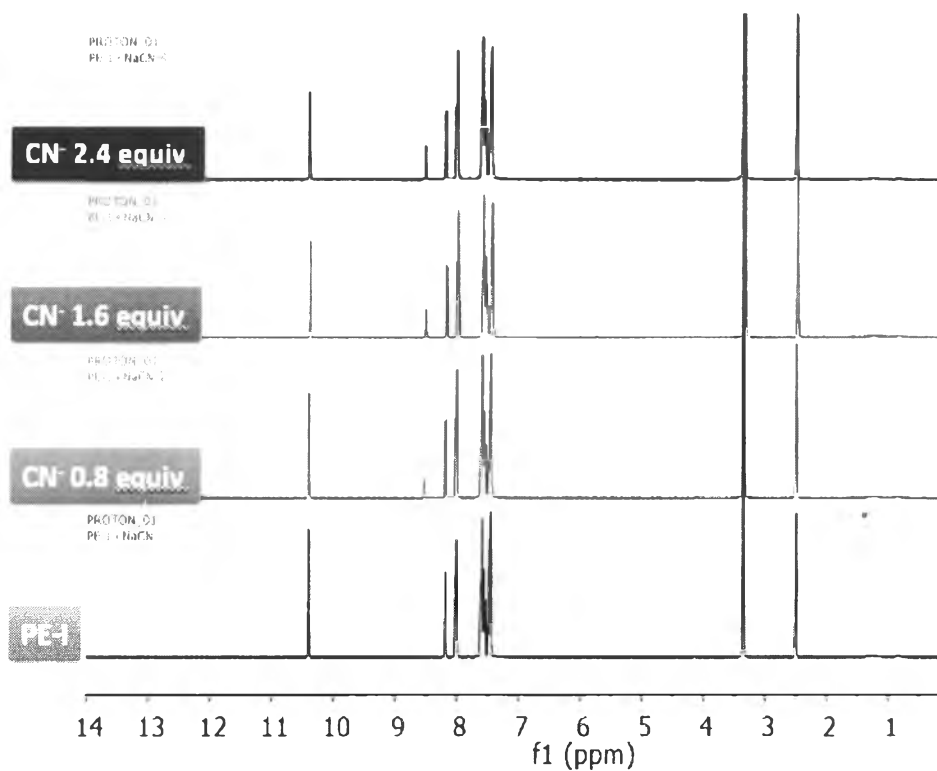


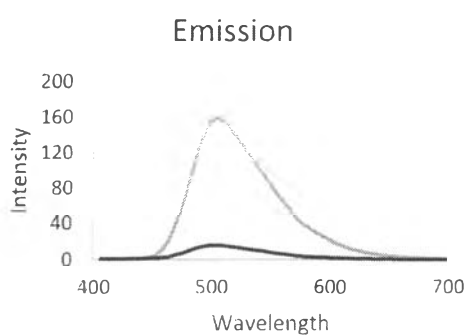
Figure 3.24  $^1\text{H-NMR}$  titration of PE I toward cyanide ion in  $\text{DMSO-d}_6$

### 3.2.3 Fluorescent sensors study of PE II

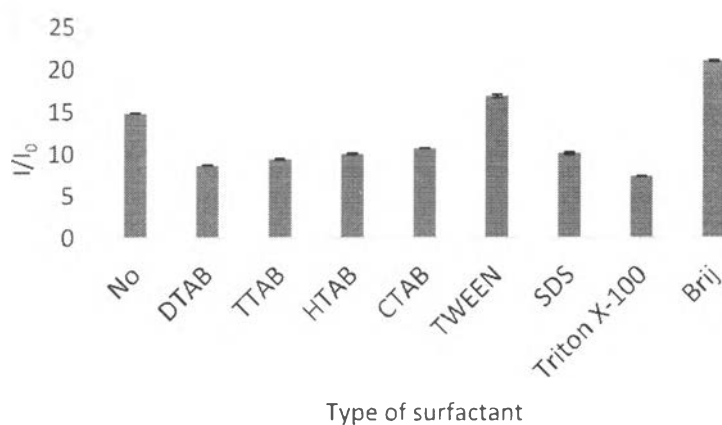
From the screening results above, The PE II showed strong fluorescence enhancement toward fluoride ion (Figure 3.25), so it further investigated the sensing ability of PE II toward fluoride ion in term of sensitivity and selectivity. Firstly, we studied the optimize condition to improve sensing ability of PE II for the detection of fluoride ion.

Because fluoride ion ( $\text{F}^-$ ) is anions belonging to halide group so it can dissolve in water, therefore we performed our measurement in a mixed solvent between aqueous buffer and DMSO, under the same condition as PE I (accomplish in HEPES buffer pH 7.4). Since it is well known that surfactants could increase the fluorescence intensity of fluorophore by reduction of aggregation and also by reduction of non-specific interactions, we therefore studied the effect surfactants to the sensing ability of PE II with fluoride ion. As expected in among all surfactant test, both the cationic

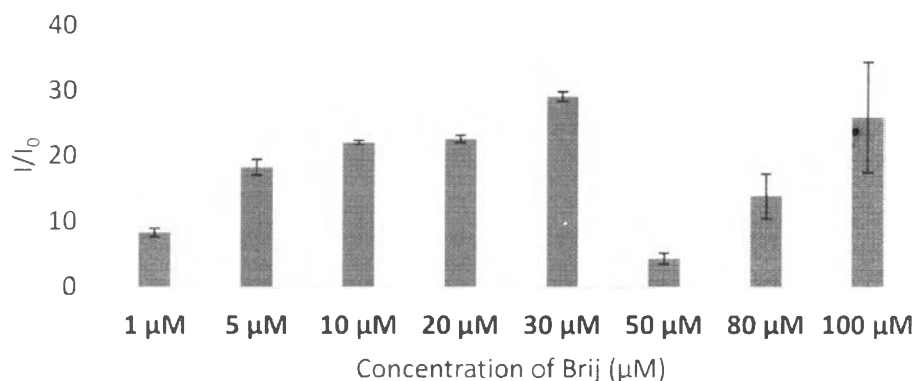
surfactants (DTAB and TTAB) and the anionic surfactant (SDS) generally gave lower sensitivity and nonionic surfactant (Brij and TWEEN20). However, among seven surfactant tested, the non-ionic surfactant Brij gave the highest sensitivity (Figure 3.26). Then, we investigated the changing in concentration of Brij as seen in Figure 3.27. The results reveal that, the concentration of DTAB at 30  $\mu\text{M}$  gave the highest fluorescence enhancement ratio (Figure 3.27).



**Figure 3.25** Emission spectrum of the solution of PE II 5  $\mu\text{M}$  upon the addition of sodium fluoride 30 eq (orange line) in 10% HEPES buffer pH 7.4/10  $\mu\text{M}$  / 90% DMSO

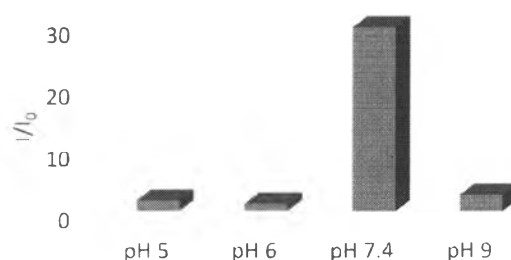


**Figure 3.26** Bar chart representing the fluorescence enhancement ( $I/I_0$ ) of PE II (5  $\mu\text{M}$ ) upon the addition of sodium fluoride (30 eq) in HEPES buffer pH 7.4 (10 mM) in the presence of various surfactants (10  $\mu\text{M}$ ).



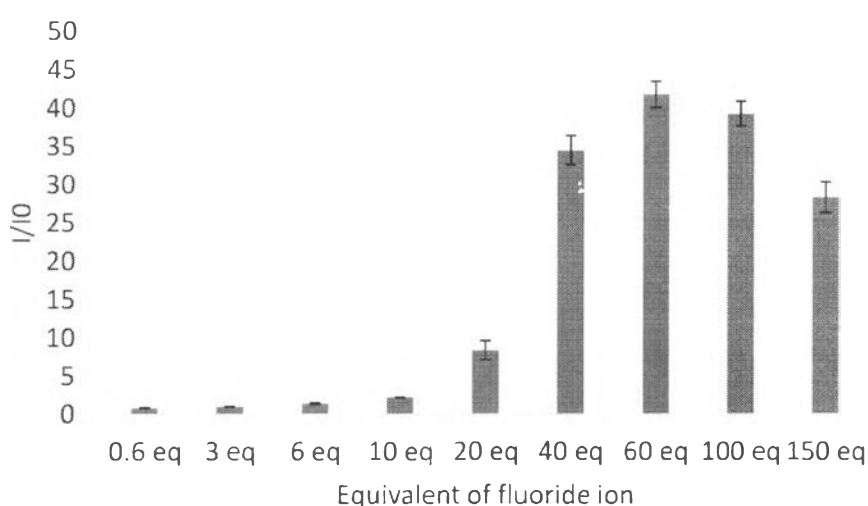
**Figure 3.27** Bar chart representing the fluorescence enhancement ( $I/I_0$ ) of PE II (5  $\mu\text{M}$ ) upon the addition of sodium fluoride (30 eq) in HEPES buffer pH 7.4 (10 mM) in the presence of various concentration of Brij.

The next parameter that we investigated is the pH. The pH variation showed effect of pH in the range of 5-9 on the fluoride sensitive (Figure 3.28). PE II was very sensitive to pH in the comparison with PE I. At neutral pH, it to give a strongest signal of fluorescence enhancement ratio ( $I/I_0$ ) around 30. However, under acidic (pH = 5-6) or basic conditions (pH = 9) the starting fluorescence signal is higher than neutral condition thus the addition fluoride ion to the system were slightly affect the fluorescence enhancement. This perhaps caused by the protonation of PE II in to aldehyde group while the deprotonation of phenolic group in PE II under the basic. Such reaction would lead to the prohibition of ICT process causing the high fluorescence intensity of the PE II.



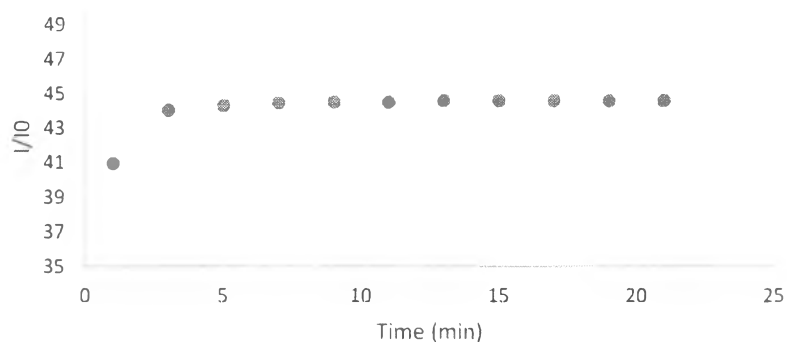
**Figure 3.28** Bar represent the fluorescence enhancement ratio ( $I/I_0$ ) of PE II 5  $\mu\text{M}$  and addition fluoride 30 eq at various pH of buffer (10  $\mu\text{M}$  in Brij (30  $\mu\text{M}$ ).

With the optimized condition in hands, the fluorescence response in relation to fluoride concentration was monitored upon the addition of various equivalents of sodium fluoride in an aqueous solvent (HEPES buffer pH 7.4, 30  $\mu\text{M}$  Brij). The fluorescence intensity initial increased almost linearly with the fluoride concentration up to 60 equivalent (300  $\mu\text{M}$ ) (Figure 3.29). It's important to note that the emission spectra were acquired at 30 minute for all sensing experiments to ascertain the complete of reaction.



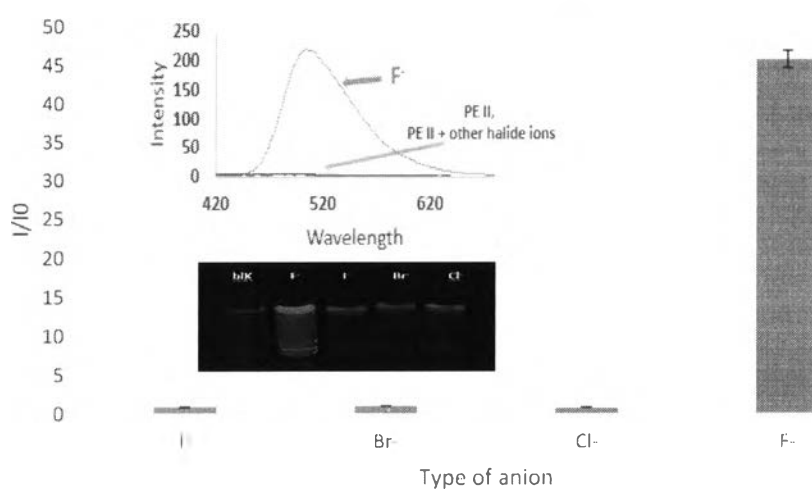
**Figure 3.29** The bars represent the fluorescence enhancement ratio ( $I/I_0$ ) of PE II (5 $\mu\text{M}$ ) at various equivalent of fluoride in Brij (30  $\mu\text{M}$ )/HEPES buffer pH 7.4 (10mM).

Then, as we realized that this fluorescence of PE II toward fluoride is a reaction mode which is time dependent and 30 minute pious the measurement might not be enough to get the highest signal enlargement. We therefor study effect of reaction time with the fluorescence intensity of PE II with fluoride ion (Figure 3.30). It shown that the fluorescence enhancement ratio were exponentially increased to 3 min and stable after that. Therefore the 5 minute measurement time were selected as optimal time for further study.



**Figure 3.30** Time-dependent changes in the fluorescence intensity of PE I (5  $\mu\text{M}$ ) upon addition of fluoride 60 equiv in Brij (20  $\mu\text{M}$ )/HEPES buffer pH 7.4 (10mM).

With the optimized condition in hands, we retest the PE II toward fluoride ion and other halide ions again using the optimal condition. The results were present in **Figure 3.31**. Upon the addition of fluoride ion at 300  $\mu\text{M}$  concentration, the fluorescence enhancement ratio were found at 45.81 while the other halide ions remain unchanged at less than 1.5. This suggest the potential use of this sensor for discrimination of fluoride ion over other halides in aqueous media.



**Figure 3.31** Fluorescence enhancement ratio ( $I/I_0$ ) of PE II 5  $\mu\text{M}$  in the presence of various halide ions (300  $\mu\text{M}$ ). The color of PE II with various halide ion under backlight (inset).

For the interference test, the selectivity test of PE II it can exhibited high specific toward fluoride ion (Figure 3.31). In addition, interference test found that other halide ion are a little bit infestation increasing fluorescence signal of PE II toward fluoride ion (Figure 3.32)

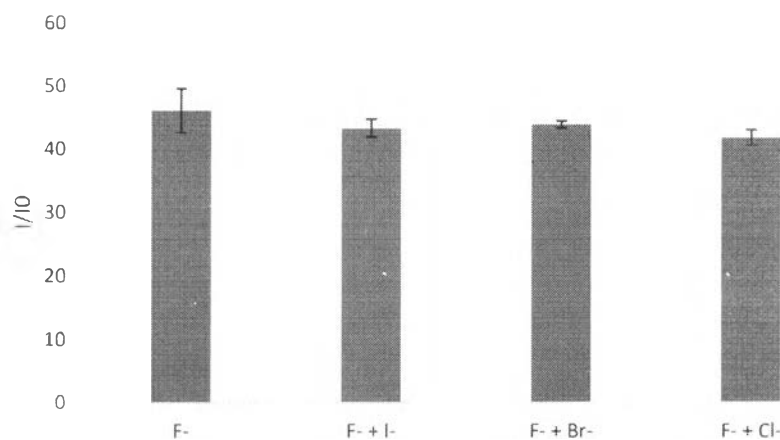


Figure 3.32 Fluorescence enhancement ratio ( $I/I_0$ ) of PE II 5  $\mu$ M in the presence of fluoride ion and another halide ion (300  $\mu$ M).

Furthermore, the determination of sensitivity is associate with the Internal Charge Transfer (ICT) process, so the fluorescence quantum yields of PE I are determine after the addition of CN<sup>-</sup> ion and fluoride ion respectively as seen in Table 3.3. It shown that the fluorescence quantum yield after addition of cyanide ion increased dramatically from 0 to 22.8 after the addition of CN<sup>-</sup> for PE I while from 0-27 after the addition of F<sup>-</sup> increase of PE II. This behavior are governed by the formation of cyanohydrin or fluorohydrin intermediate, which is not allow to the ICT process in both fluorophore.

All of these studies found that PE I and PE II can be sensor for the detection cyanide ion and fluoride ion, respectively. The observation of the starting quantum yield of PE I and PE II cannot observe (Table 3.3) because the initial intensity of PE I and PE II are very low.

**Table 3.3** Photophysical properties of PE I (5  $\mu\text{M}$ ) and PE II (5  $\mu\text{M}$ ) upon the addition of sodium cyanide (30 equiv) and sodium fluoride (60 equiv) in 10% HEPES buffer pH 7.4 10  $\mu\text{M}$ / 90% DMSO.

Compound	$I/I_0$	% $\Phi_F$	% $\Phi_F^{\text{An}}$	LOD ( $\mu\text{M}$ )
PE I	11.77	$\sim 0$	22.8	2.5
PE II	45.81	$\sim 0$	27	30

\*Quinine sulfate in 0.1 M  $\text{H}_2\text{SO}_4$  ( $\Phi_F = 0.54$ ) was the reference

